Chế tạo màng sợi nano lõi/vỏ từ chitosan, carrageenan, polyvinyl alcohol, và curcumin bằng phương pháp quay điện đồng trục hai lớp

TÓM TẮT

Phương pháp quay điện đồng trục đã được sử dụng để chế tạo thành công màng sợi nano lõi/vỏ làm từ chitosan (CS), carrageenan (CG), polyvinyl alcohol (PVA), và curcumin (CCM). Các yếu tố ảnh hưởng đến quá trình chế tạo sợi đã được khám phá, bao gồm tỷ lệ PVA/CS/CG là 8:1:1, nồng độ CG là 0,5%, khoảng cách từ đầu kim đến chất nền là 15 cm, điện áp là 18 kV và tốc độ dòng chảy là 0,1/0,1 mL/h. Các sợi nano thu được cho thấy cấu trúc lõi/vỏ rõ ràng (được quan sát thông qua ảnh TEM), với phân bố đường kính đồng đều trong phạm vi 100-600 nm, tập trung nhiều nhất trong phạm vi 100-300 nm và đường kính trung bình là 274,35 ± 19,57 nm. Dữ liệu FTIR cho thấy màng sợi PVA/CCM@PVA/CS/CG chứa các nhóm chức năng đặc trưng của CG và CCM. Kết quả giải phóng CCM trong màng sợi chứng minh rằng lượng CCM được giải phóng nhanh trong vòng 6 giờ đầu tiên. Bắt đầu từ 12 giờ, lượng CCM được giải phóng có xu hướng giảm tốc và dần ổn định, và đến 96 giờ, hàm lượng CCM được giải phóng đã đạt 83,96%. Kết quả nghiên cứu này chứng minh tiềm năng sử dụng màng nano sợi PVA/CCM@PVA/CS/CG trong quá trình lành vết thương hở.

Từ khoá: *Màng sợi nano, cấu trúc lõi/vỏ, chữa lành vết thương, chitosan, carrageenan*

Fabrication of core/shell nanofiber membrane from chitosan, carrageenan, polyvinyl alcohol, and curcumin by two-layer coaxial electrospinning

ABSTRACT

Coaxial electrospinning was used to successfully construct a core/shell nanofiber membrane made from chitosan (CS), carrageenan (CG), polyvinyl alcohol (PVA), and curcumin (CCM). Factors influencing fiber fabrication were explored, including the PVA/CS/CG ratio of 8:1:1, CG concentration of 0.5%, distance from the needle tip to the substrate to 15 cm, voltage of 18 kV, and flow rate of 0.1/0.1 mL/h. The obtained nanofibers show a distinct core/shell structure (observed by TEM image), with a uniform diameter distribution in the range of 100-600 nm, most concentrated in the range of 100-300 nm, and an average diameter of 274.35 ± 19.57 nm. The FTIR data show that the PVA/CCM@PVA/CS/CG fiber membrane contains CG and CCM-specific functional groups. The results of CCM release in the fiber membrane demonstrate that the amount of CCM released is rapid within the first 6 hours. Beginning at 12 hours, the amount of CCM released tends to decelerate and progressively stabilize, and by 96 hours, the CCM content released has reached 83.96%. This finding demonstrates the possible use of a PVA/CCM@PVA/CS/CG nanofiber membrane in open wound healing.

Keywords: *nanofiber membrane, core/shell structure, wound healing, chitosan, carrageenan*

1. INTRODUCTION

The majority of the body's structure is made up of skin, which serves as the primary protective barrier that keeps hazardous substances out. Healthy skin regulates body temperature and keeps substances in balance. However, the skin is extremely sensitive, experiencing both light touches and heavy blows. Damage to the skin affects all skin functions. The speed with which the wound heals is determined by its severity.[1]

Wound dressings play an important role in the therapy phase; selecting the proper wound dressing can save time and money. Furthermore, recent research have indicated that nanomaterials are becoming increasingly popular, with one example being wound dressings made of nanofiber membranes. Nanofibers offer several essential properties, including a tiny diameter, controllable pore size, a high surface area to volume ratio, and controlled drug release rate and time by altering the fiber structure and morphological size, resulting in excellent wound healing. As a result, nanofibers are perfect for medical applications, particularly in the fabrication of wound dressings.[2-4]

Many research initiatives have been carried out to fabricate chitosan (CS) nanofibers using the electrospinning process. Dhurai et al. (2013) used electrospinning to create nanofibers from polylactic acid (PLA) and CS that included curcumin (CCM) as a medicine. In this investigation, the CS/PLA ratio was 5.5% (w/v), CCM was 11% (w/v), and the voltage applied was 20 kV. SEM examination revealed that the average fiber diameter was 66 nm. CCM incorporated onto CS/PLA nanofilm improved antioxidant capacity while being toxicity-free.[5] In 2017, Goonoo et al. electrospun nanofibers from kappa-carrageenan (κ-CG) and fucoidan with poly(ester-ether) polydioxanone at varying ratios and solvents. The fiber mats were employed for cell culture research and tissue engineering.[6] In 2020, Madruga et al. investigated and developed biocompatible nanofibers made from a combination of polyvinyl alcohol (PVA) and carboxymethyl-kappa-carrageenan (CMKC). The aqueous solution had ratios of 1:0, 1:0.25, 1:0.4, 1:0.5, and 1:0.75 (w/w PVA:CMKC). They employed a 15 kV electric field in the electrospinning process, a 15 cm distance from the tip to the collector, and a 1 mL/h pump rate to produce nanofibers with a diameter of less than 300 nm. CMKC is anticoagulant and antibacterial against Escherichia coli and Staphylococcus aureus, as well as effective at absorbing fluids and retaining moisture. The combination of CMKC enhances cytocompatibility, biodegradability, and cell proliferation.[7] Gouda et al. effectively manufactured nanofiber membranes for wound

healing and skin regeneration using electrospinning of PVA, iota-carrageenan (ι-CG), and graphene oxide. The combination of graphene oxide and nanofibers enhances skin regeneration. Graphene-based materials have several functions, including a large surface area, protein adsorption capacity, and antibacterial qualities, hence they are utilized as wound dressings to prevent infection in diverse wounds. Many studies have shown that a tiny quantity of graphene oxide improves the attributes of polymer membranes, including mechanical strength, wound healing speed, and tissue regeneration. The membranes were examined for *Escherichia coli* and *Staphylococcus* infection. The results revealed that the membranes have good wound healing, reduce scar formation, and are antibacterial. Biopolymer-based electrospun nanofibers are extremely useful for biomedical applications.[8] In 2022, Vargas-Osorio et al. created electrospun nanofibers from polycaprolactone (PCL), CS, and κ-CG utilizing a safe solvent mixture of formic and acetic acid. The interactions of positively and negatively charged hydrophilic polysaccharides resulted in high polymer stability. All fiber mats exhibited morphological traits that indicated an average fiber diameter at the nanoscale. Investigations on living cells revealed no harmful effects; the cells multiplied and spread over time.[9]

In this study, a PVA/CCM@PVA/CS/CG nanofibrous membrane was electrospun to promote wound dressing orientation. Coaxial electrospinning was employed as a simple, one-step method for manufacturing uniformly shaped polymer fibers with core-shell structure. PVA is a promising synthetic polymer for wound dressing applications because to its biocompatibility, strong tensile and hydrophilic qualities, and fiber forming capabilities.[9-12] CS is a positively charged biopolymer produced via deacetylation of chitin.[13] CS is biodegradable, biocompatible, bactericidal, hemostatic, and has minimal toxicity, making it useful in a variety of medical applications.[14-15] CG is an anionic sulfated polysaccharide composed of galactose and anhydrogalactose units linked by glycoside linkages.[16] CG is a stabilizer, thickener, and gelling agent having numerous desired qualities in biological applications such as antiviral, anticancer, and immunomodulatory actions.[17] The combination of two oppositely charged polymers, CS and CG, was designed to optimize the nanofiber production process.[18] In addition, CCM was added to boost the membrane's antibacterial capabilities and expedite wound healing on the skin.[19-21]

2. EXPERIMENT

2.1. Chemicals

The chemicals used in this work include chitosan (CS, 92% deacetylation, Viet Nam), carrageenan (CG, Kappa-CG, Philippines), polyvinyl alcohol (PVA, 99.5%, hydrolysis degree 87 – 89%, Shanghai Zhanyun Chemical Co., China), curcumin (CCM, >90%, Viet Nam), acetic acid (AA, 90%, Xilong, China), ethanol (95%, Chemsol, Viet Nam), phosphate buffered saline (PBS, Himedia, India), Tween 20 (Guangdong, China). All other materials and reagents applied in this work were of analytical grade unless otherwise noted.

2.2. Synthesis of PVA/CCM@PVA/CS/CG nanofiber membrane

2.2.1. The shell mixture preparation

The steps to prepare CS/PVA/CCM mixture are shown in Figure 1. Firstly, to prepare a homogenous 15% PVA solution, 15 g of PVA was mixed with 100 mL of distilled water in a glass beaker and swirled on a magnetic stirrer at 80°C for 24 hours. To make a 6% CS solution, 6 g of CS was added to a glass beaker holding 100 mL of 20% AA and stirred on a magnetic stirrer at room temperature for 24 hours. A 0.5% CG solution was obtained by adding 0.5 g of CG to a glass beaker holding 100 mL of distilled water and stirring on a magnetic stirrer at 80°C for 2 hours. Finally, the PVA/CS/CG shell solution was prepared by combining PVA, CS, and CG solutions in various ratios (7:2:1, 7:1:2, and 8:1:1) and stirring for 1 hour to produce a homogenous mixture.[22-23]

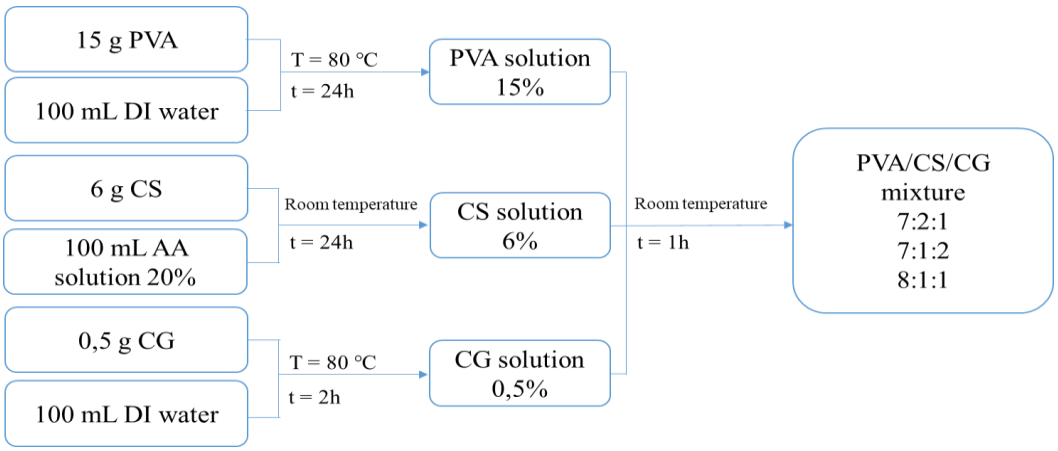

Figure 1. Flow chart of shell solution preparation process

2.2.2. The core mixture preparation

Figure 2 depicts the processes for preparing a PVA/CCM mixture. To create a 15% homogenous PVA solution, mix 15 g of PVA with 100 mL of distilled water in a glass beaker and stir with a magnetic stirrer at 80°C for 24 hours. Next, add 0.09 g of CCM to 30 mL of ethanol and stir for 1 hour at room temperature to create a CCM solution. The core solution was created by mixing the PVA and CCM solutions in an 8:2 ratio and stirring on a magnetic stirrer at room temperature for 1 hour.[22-23]

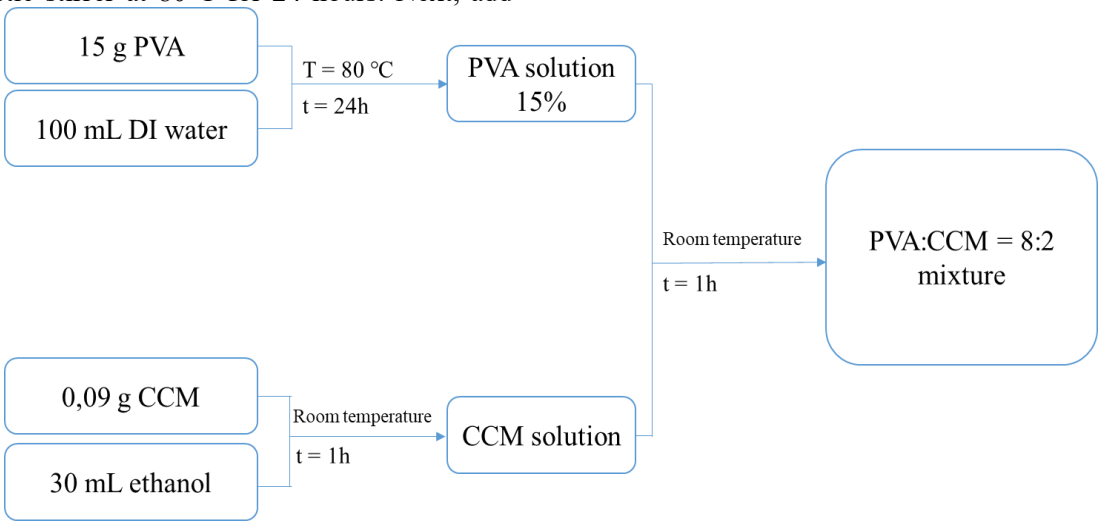

Figure 2. Flow chart of core solution preparation process

2.2.3. Nanofiber membrane processing by coaxial electrospinning

The prepared core and shell solutions were injected into two 1 mL syringes, each attached to a double-layer concentric needle, and then placed in the electrospinning equipment. The concentric needles included an outer tube with an inner diameter of 1.01 mm and an outside diameter of 1.49 mm, as well as an inner tube with an inner diameter of 0.41 mm and an outer diameter of 0.72 mm. The sample collection board was protected with aluminum foil and a voltage generator.[24-26] During the electrospinning process, the parameters were set with the sample injection flow rate at 0.1/0.1 mL/h, 0.2/0.2 mL/h, the voltage at 17 kV, 18 kV, 19 kV, and the distance from the needle tip to the sample collection was 14 cm, 15 cm, and 16 cm.

2.3. Characterisation

2.3.1. The morphology, diameter, and size distribution of nanofibers

During the pre-tests, the diameter of the nanofibers was measured using an optical microscope (Nikon EPIPHOT 200, Japan). The nanofibers accumulated immediately on the aluminum layer and were seen using a Hitachi S-4800 scanning electron microscope made in Japan. To better their observation, the nanofibers were sputter-coated with a platinum coating before being measured. The average fiber size and fiber size distribution were calculated using ImageJ software and SEM image data. The

core/shell structure of the membranes was examined using TEM (JEM-1400 Flash Jeol, Japan) in a vacuum environment. A drop of diluted sample was placed on a cellulose stub for observation.

2.3.2. Fourier transform infrared spectroscopy (FTIR)

The PVA/CCM@PVA/CS/CG nanofibrous membrane's specific functional groups were described using an FTIR instrument (Nicolet 6700, Thermo, USA). The FTIR spectra was obtained under nitrogen flow with a total of 32 scans and a 4 cm^{-1} resolution in the 4000-400 cm^{-1} wavenumber band.

2.3.3. Survey of curcumin content in fiber membrane

Establishing a standard curve for quantifying curcumin in ethanol solution

Weigh precisely 0.005 g of curcumin standard in a 100 mL volumetric flask containing ethanol solution. Pipet exactly 1 mL, 2 mL, 3 mL, 4 mL, and 5 mL of this standard solution into a 25 mL volumetric flask, filling to the mark with the same solvent. The equivalent concentrations for the five solutions above are 0.002; 0.004; 0.006; 0.008; and 0.01 mg/mL, respectively. The absorbance of solution A is measured at the wavelength λ_{max}. A graph is created using the measured values to show the connection between A and C, which yields the linear equation of A in relation to C. The equation above is used to calculate the concentration of CCM in the sample at the following stages.[22-23]

Determination of curcumin content of nanofiber membranes in ethanol solution

First, 0.005 g of the nanofiber membrane was cleaned with alcohol to remove any CCM that had adhered to the membrane's surface. The membrane was then placed in a glass beaker holding 10 mL of ethanol solution. The beaker was sonicated at predefined time intervals (15, 30, 45, and 60 minutes). At these time points, 2 mL of the sample was removed for analysis, and 2 mL of fresh ethanol was added. The 2 mL of extracted material was combined with 8 mL of ethanol before UV-Vis analysis to quantify the amount of CCM released.

2.3.4. Investigation of curcumin release process

Establishing a standard curve for quantifying curcumin in buffer solution

Weigh exactly 0.005 g of curcumin standard in a 100 mL volumetric flask containing a 4:1 mixture of ethanol solution and PBS buffer solution. Pipette exactly 1 mL, 2 mL, 3 mL, 4 mL, and 5 mL of this standard solution into a 25 mL volumetric flask, filling to the mark with the same solvent. The equivalent concentrations for the five solutions above are 0.002; 0.004; 0.006; 0.008; and 0.01 mg/mL, respectively. The absorbance of these solutions is measured at the maximum wavelength (λ_{max}). A graph is created using the measured values to show the connection between A and C, which yields the linear equation of A in relation to C. The equation above is used to calculate the concentration of CCM in the sample at each stage. The amount of CCM released for each survey period can be calculated using the standard curve equation described above.

Experimental release of curcumin in buffer solution

To imitate the animal serum environment, 0.005 g of nanofiber membrane was cleaned with alcohol before being placed in a glass beaker with 10 mL of PBS solution (pH 7.4) and 1% tween 20. The beakers were kept at a temperature of 37 ± 1°C using a thermostat. Next, at certain time intervals (5 minutes, 10 minutes, 15 minutes, 30 minutes, 1 hour, 2 hours, 3 hours, 4 hours, 6 hours, 12 hours, 24 hours, 48 hours, 72 hours, and 96 hours), 2 mL of sample was removed for analysis and 2 mL of new buffer was added. 2 mL of the analyzed sample was mixed with 8 mL of ethanol solution before being analyzed using a UV-Vis spectrometer to determine the amount of released CCM. Therefore, the percentage of CCM drug released from the fiber membrane can be calculated.[22]

3. RESULTS AND DISCUSSION

3.1. Results on the influence of some factors on the electrospinning process

3.1.1. Effect of PVA/CS/CG ratio

PVA, CS, and CG solutions were made and combined in the following ratios: 7:2:1, 7:1:2, and 8:1:1 to study the effect of the PVA/CS/CG ratio. Figure 3 depicts the survey results as observed via an optical microscope. The results demonstrate that in Figure 3a, there are many individual particles and fiber particles, but no full fibers are created. When the CG ratio is increased in the solution in Figure 3b, it is noted that there are less individual particles, more fiber particles, and fibers without particles; however, these fibers are not continuous but rather fractured. Furthermore, the PVA ratio utilized in the electrospinning solution is insufficient to draw full fibers, so adding more CG to the fiber does not result in

continuous formation. In Figure 3c, the PVA ratio is raised, and no more particles or fiber particles occur; instead, the fiber is created continuously and without breaking. The addition more amount of CG (ratios of 7:1:2 and 7:2:1) increases the conductivity of electrospun solutions[27], resulting in stronger repulsive forces between the charged polymer groups, which enhances the elongation forces during eletrospinning, resulting in thinner fiber with breaking formation. These findings indicate that the 8:1:1 PVA/CS/CG ratio produces a desirable fiber morphology, making it the optimized proportion for incorporating CG into the nanofiber system.

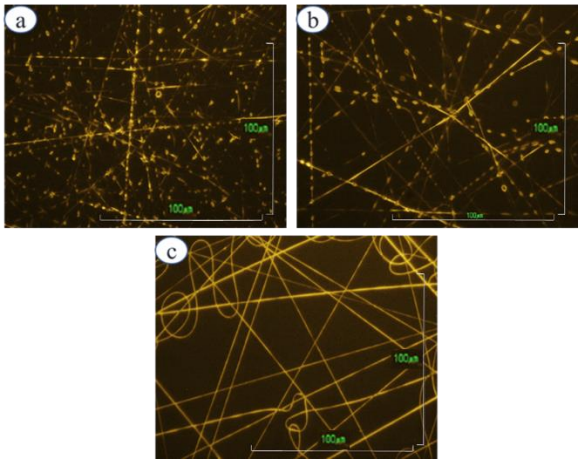

Figure 3. Optical microscope images of polymer fibers corresponding to PVA:CS:CG ratios of (a) 7:2:1, (b) 7:1:2, and (c) 8:1:1

3.1.2. Effect of carrageenan concentration

Optical microscopy photos (Figure 4) reveal that CG at a concentration of 0.3% forms fibrils, however the fibrils are intermingled with particles, resulting in the creation of granular fibers. When the CG concentration is increased to 0.5%, the resulting fibers are more homogeneous, straight, and continuous. At a CG concentration of 0.7%, the fibers generated have a smaller diameter due to enhanced conductivity in the solution; however, the fibers are not continuous and are fragmented into pieces, resulting in granular fibers. Chitosan is a polycation, which can form ion complexes with a variety of natural or manufactured anions, including the polymer carrageenan. Because the presence of amino groups in the CS structure increases the surface tension of the solution, the use of two types of polymers with opposite charges has resulted in positive charges in the CS structure and negative charges in the CG structure interacting with each other, and at a CG concentration of 0.5%, these charges are neutralized, resulting in straight and smooth nanofibers. Therefore, the electrospinning process uses a CG concentration of 0.5%.

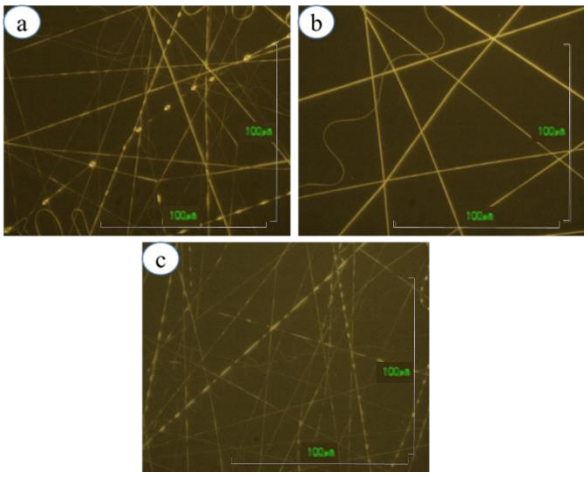

Figure 4. Optical microscope images of polymer fibers corresponding to CG concentrations: (a) 0.3%, (b) 0.5%, and (c) 0.7%

3.1.3. Effect of sampling distance

Figure 5 depicts the optical microscope results, which demonstrate clear changes in the fibers at distances of 14 cm, 15 cm, and 16 cm. At a distance of 14 cm, the fibers generated are relatively big, discontinuous, and frequently curved. When the distance between the nozzle tip and the sample collector is increased to 15 or 16 cm, the fiber size decreases. This can be explained by the fact that at a greater distance, the solvent has more time to evaporate, resulting in fibers with smaller diameter. The longer the distance, the more evenly distributed the fibers on the sample collector. Furthermore, particles will be created at both too close and too far away distances. The fibers have generally consistent diameters, are straight, and continuous over a distance of 15 cm, therefore this is the ideal distance for the electrospinning process.

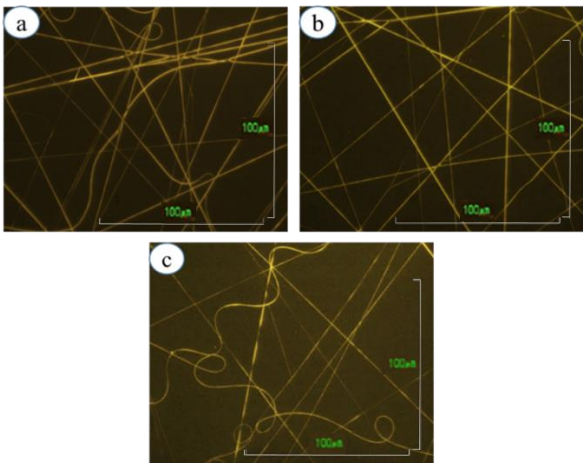

Figure 5. Optical microscope images of polymer fibers corresponding to fiber forming distances of: (a) 14 cm, (b) 15 cm, and (c) 16 cm

3.1.4. Effect of applied voltage

Voltage is critical in the electrospinning process because it regulates the electric field intensity between the needle tip and the sample collection. Figure 6 illustrates how voltage affects the electrospinning process for voltage values of 17 kV, 18 kV, and 19 kV. In general, fiber size reduces as voltage increases; at 17 kV, the fibers generated have a rather wide diameter, are irregular, and tend to cling together. This is because, at low voltage, the primary droplet's electrostatic repulsion is insufficient to overcome the solution's surface tension. Furthermore, at low voltage values, the solvent in the solution evaporates slowly, preventing the fibers from drying before reaching the sample collector. When the voltage is increased to 18 kV, the fibers form with a reasonably homogeneous and smaller diameter, and they are straight and continuous. When the voltage was increased to 19 kV, the fiber diameter reduced, but it was fractured and not uniform. Because of the high voltage, the solvent molecules rubbed fast, causing the solution to dry quickly at the primary drop at the nozzle tip. The dry main drop interrupted the electrospinning process, causing the fibers to break and bend, perhaps leading to a complete cessation of the electrospinning process.

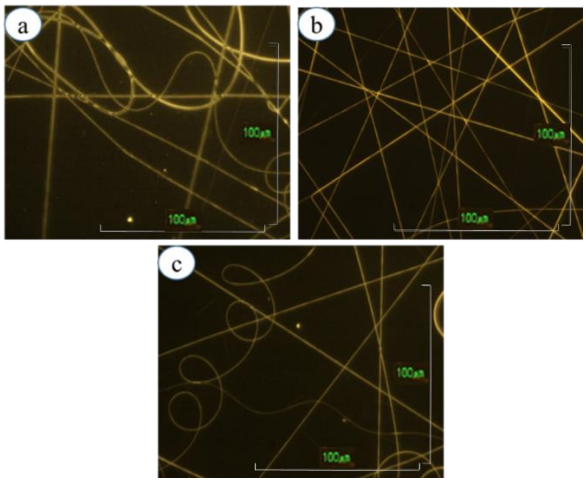

Figure 6. Optical microscope images of polymer fibers corresponding to the voltages: (a) 17 kV, (b) 18 kV, and (c) 19 kV

3.1.5. Effect of injection flow

Figure 7 depicts the results of the inquiry into the effect of injection flow rate on the electrospinning process. It was discovered that when the injection flow rate was 0.1/0.1 mL/h, the fibers developed constantly. When the injection flow rate was increased to 0.2/0.2 mL/h, the fibers condensed and bent, forming beads. Because of the increased injection flow rate, more solution was pushed out, leaving insufficient time for the solvent to evaporate, resulting in the primary droplet at the injection tip progressively growing larger over time and eventually dripping down to the sample collector. Droplet dripping interrupts the electrospinning process, resulting in fibers with irregular diameters and even beads. As a result, the flow rate used for the electrospinning operation was 0.1/0.1 mL/h.

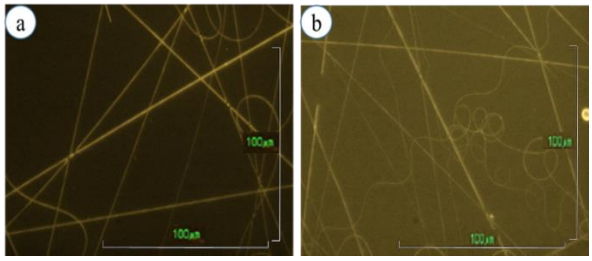

Figure 7. Optical microscope images of polymer fibers corresponding to injection flow rates of: (a) 0.1/0.1 mL/h and (b) 0.2/0.2 mL/h

3.2. Physiochemical characteristics of nanofiber membrane

3.2.1. Fiber morphology results by SEM and TEM analysis

Figure 8 depicts a SEM picture of the PVA/CCM@PVA/CS/CG membrane under optimum circumstances. The PVA/CS/CG ratio is 8:1:1, the CG concentration is 0.5%, the distance between the needle tip and the sample collector is 15 cm, the electrospinning voltage is 18 kV, and the spray flow rate is 0.1/0.1 mL per hour. The SEM image results demonstrate that there are no particles on the fiber surface, indicating that the substances have completely dissolved and the polymer solution mixture is homogeneous. Moreover, the TEM images revealed obvious core-shell structure of the nanofibers, with a light shell layer coating around the dark core. The core/shell structure of nanofiber structures aids in the controlled release of healing agents (curcumin), promoting effective wound healing compared to single-layer nanofibers. Additionally, ImageJ software is used to determine the size of the fibers in the SEM picture, and a fiber diameter distribution chart is created from this information. The graph illustrates the distribution of fiber diameter, which is in the range of 100 - 600 nm, with the highest concentration in the range of 100 - 300 nm and an average diameter of 274.35 ± 19.57 nm. In addition, when compared with the nanofibers prepared by Cao-Luu et al. (2024), the PVA/CCM@PVA/CS/CC fiber has an average diameter of 301.55 ± 76.77 nm, indicating that the PVA/CCM@PVA/CS/CG nanofiber has a smaller diameter.[22] The combination of two types of

charged polymers helps increase the conductivity of the solution, contributing to the fiber diameter reduction. This has demonstrated the efficiency of combining two types of polymers with opposite charges to produce nanofibers using the electrospinning technique.[23]

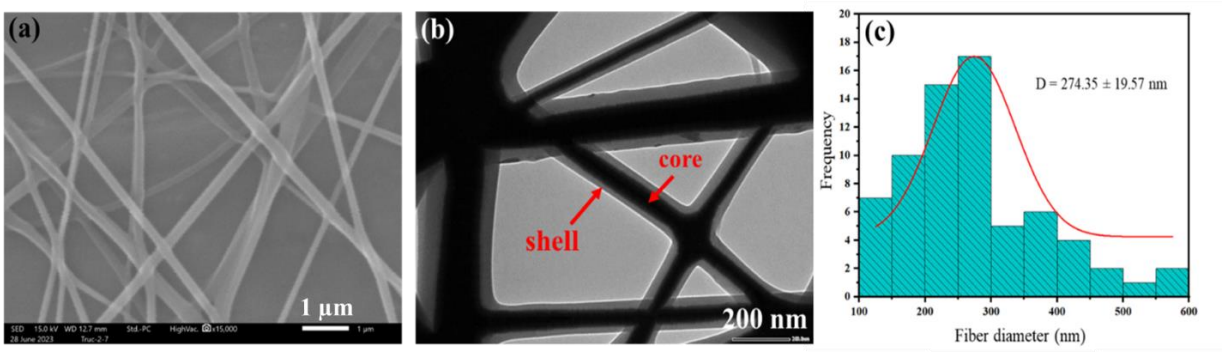

Figure 8. Morphology of nanofiber membranes through (a) SEM image, (b) TEM image, and (c) fiber diameter distribution histogram

3.2.2. FTIR results of the nanofiber membrane

The chemical properties of PVA/CCM@CS/PVA/CC nanofibrous membrane were determined using FTIR analysis, which revealed interactions between functional groups present in the nanofibers (Figure 9). The absorption peak at 3505 cm^{-1} in CCM's FTIR spectrum corresponds to the stretching vibration of (O-H). The range from 3100 to 2800 cm^{-1} corresponds to the stretching vibration of (C-H), specifically the asymmetric stretching vibration of (C-H) in (-CH_2-), as demonstrated by the peak at 2945 cm^{-1}. The peak at 1626 cm^{-1} arises owing to the stretching vibration of (C=O) and (C=C), whereas the peak at 1603 cm^{-1} is due to the stretching vibration of (C=C) and the benzene ring. The peak at 1508 cm^{-1} corresponds to a stretching vibration within the benzene ring. The peaks at 1427 cm^{-1} and 1377 cm^{-1} represent the bending and stretching vibrations of (C-H), respectively. The peaks at 1275 cm^{-1}, 1152 cm^{-1}, 1026 cm^{-1}, 961 cm^{-1}, and 856 cm^{-1} represent the stretching vibration of (C–O).

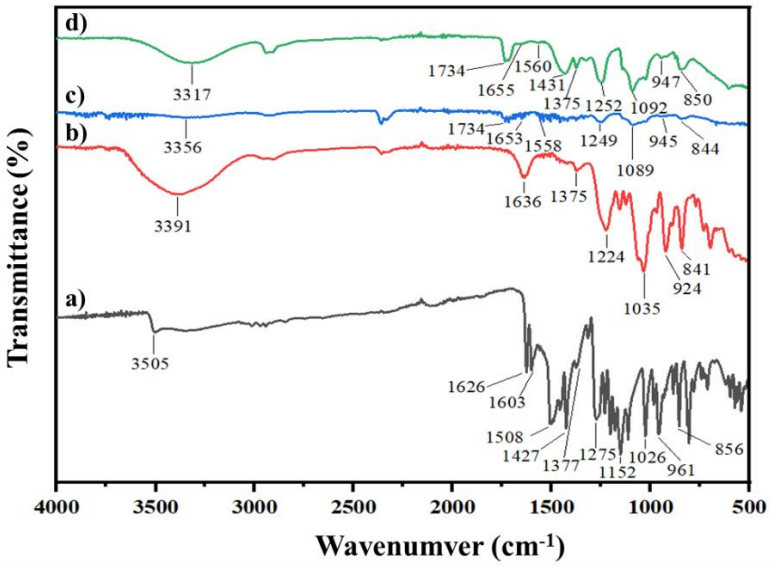

Figure 9. FTIR spectra of (a) CCM, (b) CG, (c) PVA/CS/CG, and (d) PVA/CCM@PVA/CS/CG

The FTIR spectrum of CG displays a large region in the range of 3600-3100 cm^{-1}, with the peak at 3391 cm^{-1} representing the stretching vibration of (O-H) from the hydroxyl group of the polysaccharide, which corresponds to the hydrophilic nature. The spectra reveals a peak at 2903 cm^{-1}, which corresponds to the symmetric stretching vibration of C-H. The 1636 cm^{-1} peak corresponds to the stretching of (C=O) and (C=C). The characteristic peak at 1375 cm^{-1} is caused by the stretching vibration of (C-H), whilst the high absorption peak at 1224 cm^{-1} is caused by the presence of (S=O) bonds in the sulfate ester groups. The CG spectrum displays a strong absorption peak in the range of 1020 - 1050 cm^{-1}, which is characteristic of polysaccharides, with

the peak at 1035 cm^{-1} corresponding to the stretching vibration of (C-O). The peak at 922 cm^{-1} represents the (C-O-C) bond of 3,6-anhydro-D-galactose. The signal at 841 cm^{-1} indicates the presence of (C-O-SO_3-)-D-galactose-4-sulfate. This shows the presence of κ-CG.

The FTIR spectrum of the PVA/CS/CG film shows a peak at 3356 cm^{-1}, which corresponds to the stretching vibration of two groups: hydroxyl (O-H) in PVA, CS, and CG and amino group (N-H) in CS. They have changed to lower wavenumbers, indicating that cross-linking has occurred between the groupings. The absorption peak at 2908 cm^{-1} corresponds to the symmetric stretching vibration of (C-H) in (-CH_2-). The peak at 1734 cm^{-1} represents the stretching vibration of the (C=O) group in amide I; its appearance is related to bond overlap when compared to the peak at 1626 cm^{-1} (C=O) group of CCM and the peak at 1636 cm^{-1} (C=O) of CG. The peak at 1653 cm^{-1} corresponds to the stretching vibration of the (C=O) group in amide I, while the bending vibration (N-H) of the N acetyl group in amide II has a characteristic peak at 1558 cm^{-1} associated with CS. The peak at 1375 cm^{-1} indicates the stretching vibration of (C-H), whereas the peak at 1224 cm^{-1} in the CG spectrum moves to the peak at 1249 cm^{-1}, which corresponds to the (S=O) bond in the sulfate ester groups. The peak at 1089 cm^{-1} is caused by the stretching of the (C-O) bond and the bending of the (O-H); also, this peak demonstrates the merging and overlap of the (C-O) bond when compared to the peak at 1035 cm^{-1} (of CG). Furthermore, the signal at 1089 cm^{-1} corresponds to the free amino groups at the C2 position of glucosamine. The peaks at 922 cm^{-1} and 841 cm^{-1} that correspond to the (C-O-C) bond and the presence of (C-O-SO_3-) in CG shifted to the peaks at 945 cm^{-1} and 844 cm^{-1}.

The peak 3317 cm^{-1} in the FTIR spectrum of the PVA/CCM@PVA/CS/CG film is the merger of the peaks 3505 cm^{-1} (in CCM), 3391 cm^{-1} (in CG), and 3356 cm^{-1} (in PVA/CS/CG film), which is caused by the stretching of the (O-H in PVA, CS, and CG) and amino groups (N-H in CS). The peak 2910 cm^{-1}, which has shifted from the peak 2908 cm^{-1} in PVA/CS/CG, is a merger of the peaks 2945 cm^{-1} (in CCM) and 2903 cm^{-1} in CG, both of which are indicative of the stretching vibration of (C-H). The amide group shifts the peak 1653 cm^{-1} (of the PVA/CS/CG membrane) to 1655 cm^{-1}, and the peak 1558 cm^{-1} shifts to 1560 cm^{-1}. Furthermore, the 1427 cm^{-1} peaks, which correspond to the bending vibration of (C-H) in (-CH_3), migrated to 1431 cm^{-1} and 1375 cm^{-1}. The peaks 1427 cm^{-1} and 1377 cm^{-1} in CCM, as well as the peak 1375 cm^{-1} in CG, merged to form the peak 1375 cm^{-1} characteristic of the alkane group (C-H). The change in intensity of this band is caused by PVA and CG's tendency to bind with water and hydroxyl groups present in CS and CCM, resulting in the shift of these peaks. The PVA/CS/CG membrane's peaks at 1249 cm^{-1} and 1089 cm^{-1} changed to 1252 cm^{-1} and 1092 cm^{-1}, respectively. The typical peaks for the presence of CG in the PVA/CS/CG membrane were 945 cm^{-1} and 844 cm^{-1}, which were shifted to 947 cm^{-1} and 850 cm^{-1}, respectively, and the shifts of these peaks were likewise connected to the CCM (C-O) groups. The movements of the hydroxyl, amide, and sulfate groups revealed bond overlap and the development of polyanion-cation complexes.

FTIR research revealed a successful combination of PVA, CS, CG, and CCM in the electrospinning process for fiber membranes. The spectrum revealed the presence of specific functional groups in the fiber membranes, particularly CG's sulfate group. These findings demonstrated the creation of nanofibers between two polysaccharides with opposing charges, CS and CG.

3.3. Results of CCM content in fiber membrane

3.3.1. Establish the CCM standard curve in ethanol solution

First, the maximum absorption spectrum of CCM in ethanol was set to estimate the maximum absorption wavelength of CCM, and then create the absorption standard curve for CCM. The UV-Vis spectrum data indicate that CCM's maximum absorption wavelength in ethanol solution is 426 nm.

Table 1. Absorption of CCM in ethanol solution with different concentrations

CCM content (mg/L)	Absorbance in ethanol solution	Absorbance in PBS buffer solution
0	0	0
2	0.2736	0.2741
4	0.6098	0.6727

6	0.8557	0.9257
8	1.1878	1.2585
10	1.5112	1.5896

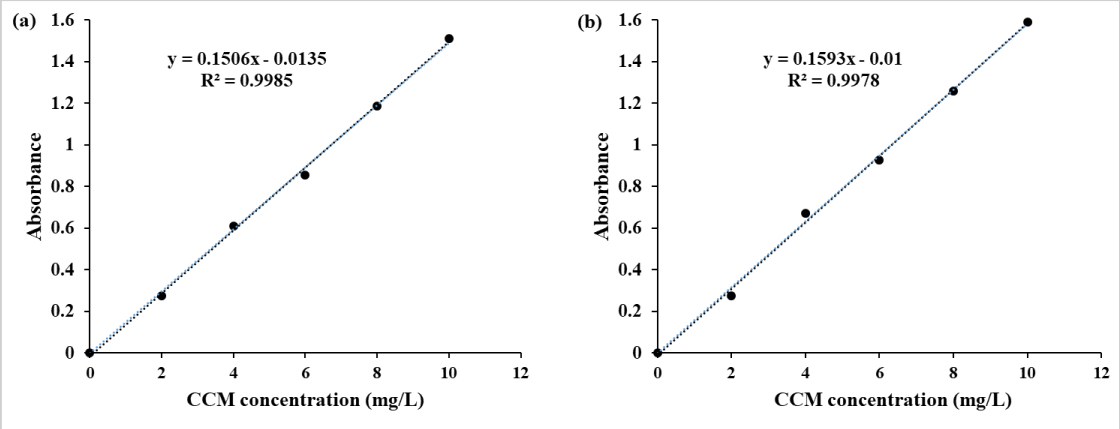

Figure 10. Standard curve of CCM (a) in ethanol solution, and (b) in PBS buffer solution

Based on the results in Table 1, a CCM standard curve in ethanol solution was created and shown in Figure 10.

The standard equation for CCM in ethanol solution is y = 0.1506x - 0.0135, where y is the absorbance and x is the CCM content (mg/L). This equation is used to calculate the CCM content released based on the ultrasonic time. Results of the ultrasonic time survey to determine the curcumin content.

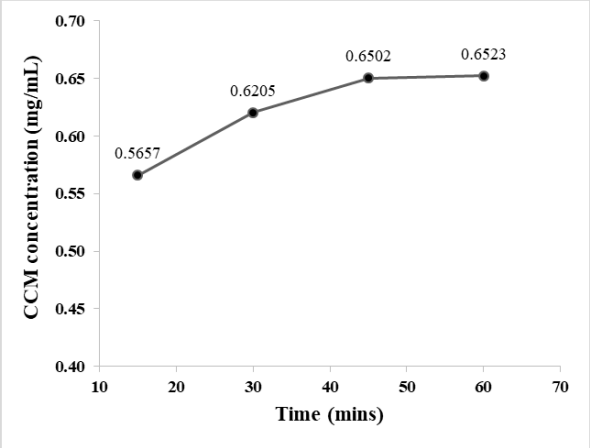

Figure 11. Ultrasonic time survey chart for determining CCM content

The CCM content released at varied ultrasonication durations of 15, 30, 45, and 60 minutes was estimated using the UV-Vis analysis results and the standard curve equation, and is shown in Figure 11. The results showed that the CCM content released was 0.5657 mg within the first 15 minutes and 0.6205 mg after 30 minutes. When the period was extended to 45 minutes, the CCM content released was 0.6502 mg. There was no substantial difference in the CCM content released at 45 and 60 minutes. As a result, the best time for ultrasonic testing was 60 minutes.

3.4. Results of curcumin release process

Establish the standard curve equation for curcumin in buffer solution.

According to the UV-Vis spectrum measurements, the maximum absorption wavelength of CCM in buffer solution is 426 nm. The standard curve equation for CCM in buffer solution is y = 0.1593x - 0.01, where y is absorbance and x is the CCM concentration in ethanol solution (mg/L). The standard curve equation can be used to compute the CCM content released throughout the *in vitro* process, as well as the percentage of CCM released with time.

Curcumin release results

Table 2 and Figure 12 shows the results of the CCM release process in the buffer solution of the PVA/CCM@PVA/CS/CG fiber membrane. Because PVA, CS, and CG can all absorb water, causing the fibers to inflate, the solution from the release media quickly reaches the core of the fiber, resulting in fast diffusion of CCM molecules within the first 6 hours after placing the membrane in the release medium. Starting at 12 hours, the amount of CCM released tends to slow and eventually settle. By 96 hours, 83.96% of the CCM content has been released. CCM released early in the process aids in anti-inflammation, whereas CCM released later aids in anti-oxidation and wound healing.

Table 2. Percentage of CCM released in buffer solution

Time (hours)	Percentage of CCM released
0.08	18.48 ± 1.92
0.17	24.99 ± 2.47
0.25	31.60 ± 2.34
0.50	41.46 ± 2.26
1	51.19 ± 2.09
2	62.26 ± 1.01
3	72.12 ± 1.48
6	77.56 ± 1.43
12	78.83 ± 2.19
24	81.54 ± 2.29
48	82.55 ± 2.16
72	83.89 ± 2.26
96	83.96 ± 2.29

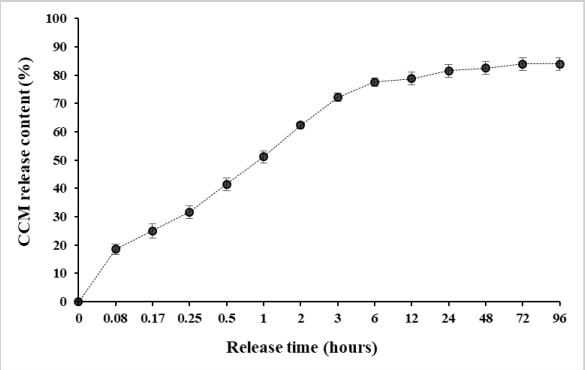

Figure 12. CCM release results of PVA/CCM@PVA/CS/CG fibers in 96 hours

4. CONCLUSION

PVA/CCM@PVA/CS/CG nanofiber membranes were produced using the following optimum ratios: The PVA:CS:CG ratio was 8:1:1, the CG concentration was 0.5%, the distance between the needle tip and the sample collector was 15 cm, the electrospinning voltage was set at 18 kV, and the spray flow was 0.1/0.1 mL/h. The produced fibers were relatively consistent in size, with diameters ranging from 100 to 300 nm and an average diameter of 274.35 ± 19.57 nm. The FTIR data revealed the presence of PVA, CS, CG, and CCM in the fiber membrane, as well as the fact that the connection between CG and CS and the structure of CCM did not change during the electrospinning process used to create nanofiber membranes. The drug release data showed that CCM was released in substantial levels in the first 6 hours, then steadily dropped after 12 hours, and by 96 hours, the amount of CCM released was 83.96%.

REFERENCES

1. A. J. Hassiba, , M. E. E. Zowalaty, G. K. Nasrallah, T. J. Webster, A. S. Luyt, A. M. Abdullah, A. A. Elzatahry. Review of Recent Research on Biomedical Applications of Electrospun Polymer Nanofibers for Improved Wound Healing, *Nanomedicine*, **2016**, *11*(6), 715–737.

2. S. Enoch, D. J. Leaper. Basic science of wound healing, *Surgery (Oxford)*, **2008**, *26*(2), 31-37.

3. M. Liu, X.-P. Duan, Y.-M. Li, D.-P. Yang, Y.-Z. Long. Electrospun nanofibers for wound healing, *Materials Science and Engineering: C*, **2017**, *76*, 1413-1423.

4. J. Lei, L. Sun, P. Li, C. Zhu, Z. Lin, V. Mackey. The wound dressings and their applications in wound healing and management, *Health Science Journal*, **2019**, *13*(4), 1-8.

5. B. Dhurai, N. Saraswathy, R. Maheswaran et al. Electrospinning of curcumin loaded chitosan/poly (lactic acid) nanofilm and evaluation of its medicinal characteristics, *Front. Mater. Sci.*, **2013**, *7*, 350–361.

6. N. Goonoo, A. Bhaw-Luximon, G. L. Bowlin, D. Jhurry. Enhanced differentiation of human preosteoblasts on electrospun blend fiber mats of polydioxanone and anionic sulfated polysaccharides, *ACS Biomaterials Science & Engineering*, **2017**, *3*, 3447–3458.

7. L. Y. C. Madruga, R. C. Balaban, K. C. Popat, M. J. Kipper. Biocompatible Crosslinked Nanofibers of Poly(Vinyl Alcohol)/Carboxymethyl-Kappa-Carrageenan Produced by a Green Process, *International Journal of Advanced science news*, **2020,** *21*(1), 2000292.

8. M. H. Gouda, S. M. Ali, S. S. Othman, S. A. Abd Al-Aziz, M. M. Abu-Serie, N. A. Elsokary, N. A. Elessawy. Novel scafold based graphene oxide doped electrospun iota carrageenan/polyvinyl alcohol for wound healing and pathogen reduction: in-vitro and in-vivo study, *Scientific reports*, **2021**, *11*, 20456.

9. Z. Vargas-Osorio, F. Ruther, S. Chen, S. Sengupta, L. Liverani, M. Michálek, D. Galusek, A. R. Boccaccini. Environmentally friendly fabrication of electrospun nanofibers made of polycaprolactone, chitosan and κ-carrageenan (PCL/CS/κ-C), *Biomedical Materials*, **2022**, *17*, 045019.

10. T. S. Gaaz, A. B. Sulong, M. N. Akhtar, A. A. H. Kadhum, A. B. Mohamad, A. A. Al-Amiery. Properties and Applications of Polyvinyl Alcohol, Halloysite Nanotubes and Their Nanocomposite, *Molecules*, **2015**, *20*(12), 22833-22847.

11. S. Ram, T. K. Mandal. Photoluminescence in small isotatic, atactic and syndiotactic PVA polymer molecules in water, *Chemical Physics*, **2004**, 121-128.

12. B. Schon, S. Monika. Electrospinning of Polyvinyl alcohol Based Wound Dressing. *Universidade de Lisboa (Portugal) ProQuest Dissertations & Theses*, **2019**.

13. V. Zargar, M. Asghari, A. Dashti. A Review on Chitin and Chitosan Polymers: Structure, Chemistry, Solubility, Derivatives, and Applications, *ChemBioEng Reviews*, **2014**, *2*(3), 204-266.

14. H. M. Ibrahim, E. M. R. EI-Zairy. Chitosan as a Biomaterial – Structure, Properties and Electrospun Nanofibers, *Concepts, compounds and the alternatives of antibacterials,* **2014**.

15. M. A. Ibrahim, M. H. Alhalafi, E. A. M. Emam, H. Ibrahim, R. M. Mosaad, A review of Chitosan and Chitosan Nanofibers: Preparation, Characterization, and Its Potential Applications. *Polymers* **2023**, *15*(13), 2820.

16. J. Guan, L. Li, S. Mao. Applications of Carrageenan in Advanced Drug Delivery, *Seaweed Polysaccharides: Isolation, Biological and Biomedical Applications*, **2017**, 283-303.

17. B. Neamtu, A. Barbu, M. O. Negrea, C. Ș. Berghea-Neamțu, D. Popescu, M. Zăhan, V. Mireșan. Carrageenan-Based Compounds as Wound Healing Materials. *International Journal of Molecular Science*, **2022**, *23*(16), 9177.

18. S. S. Biranje, P. V. Madiwale, K. C. Patankar, R. Chhabra, P. Bangde, P. Dandekar, R. V. Adivarekar. Cytotoxicity and hemostatic activity of chitosan/carrageenan composite wound healing dressing for traumatic hemorrhage, *Carbohydrate Polymers*, **2020**, *239*, 116106.

19. S. I. Sohn, A. Priya, B. Balasubramaniam. Biomedical Applications and Bioavailability of Curcumin – An Updated Overview, *Pharmaceutics*, **2021**, *13*(12), 2102.

20. S. Mitra, T. Mateti, S. Ramakrishna, A. Laha. A Review on Curcumin-Loaded Electrospun Nanofibers and their Application in Modern Medicine, *Interactions between Biomaterials and Biological Tissues and Cells*, **2022**, *74*, 3392-3407.

21. A. Kumari, N. Raina, A. Wahi, K. W. Goh, P. Sharma, R. Nagpal, A. Jain, L. C. Ming, M. Gupta. Wound-Healing Effects of Curcumin and Its Nanoformulations: A Comprehensive Review, *Pharmaceutics*, **2022**, *14*(11), 2288.

22. N. H. Cao-Luu, H. V. T. Luong, T. V. Nguyen, B. T. Nguyen-Thi, D. T. Pham, N. C. Pham, M. H. Ho. Curcumin-Loaded Co-Axial Electrospun Chitosan/Polyvinyl Alcohol/Calcium Chloride Nanofibrous Membranes for Wound Healing Enhancement, *ChemistrySelect*, **2024**, *9*(38), e202402644.

23. C. L. N. Hanh, N. T. B. Thuyen, N. T. Vy, N. T. N. Mai, N. T. Ty. Fabrication of electrospun chitosan/polyvinyl alcohol membranes with antibacterial ability to aid in the open wound healing**,** *CTU Journal of Innovation and Sustainable Development*, **2024** (Accepted).

24. X. Liu, H. Xu, M. Zhang, D. G. Yu. Electrospun Medicated Nanofibers for Wound Healing: Review, *Membranes*, **2011**, *11*(10), 770.

25. A. Al-Abduljabbar, I. Farooq. Electrospun Polymer Nanofibers: Processing, Properties, and Applications, *Polymers*, **2022**, *15*(1), 65.

26. A. Memic, T. Abdullah, H. S. Mohammed, K. J. Navare, T. Colombani, S. A. Bencherif. Latest Progress in Electrospun Nanofibers For Wound Healing Applications, *ACS Applied Bio Materials*, **2019**, *2*(3), 952-969.

27. Z. P. Rad, J. Mokhtari, M. Abbasi. Fabrication and characterization of PCL/zein/gum arabic electrospun nanocomposite scaffold for skin tissue engineering, *Materials Science and Engineering: C*, **2018**, *93*, 356-366.